Mean-field dynamics of the spin-magnetization coupling in ferromagnetic materials:
Application to current-driven domain wall motions

Jingrun Chen[1], Carlos J. García-Cervera[1,2], and Xu Yang[1]

[1]Department of Mathematics, University of California, Santa Barbara, CA 93106, USA
[2]Visiting Professor at BCAM – Basque Center for Applied Mathematics, Mazarredo 14, E48009 Bilbao, Basque Country – Spain

In this paper, we present a mean-field model of the spin-magnetization coupling in ferromagnetic materials. The model includes non-isotropic diffusion for spin dynamics, which is crucial in capturing strong spin-magnetization coupling. The derivation is based on a moment closure of the quantum spinor dynamics, coupled to magnetization dynamics via the Landau-Lifchitz-Gilbert equation and the spin transfer torque. The method is general and systematic, and can be used to study spin-orbit coupling as well. The form of the non-isotropic diffusion is generic, i.e., independent of the closure assumptions. Fully three-dimensional numerical simulation is implemented and applied to predict current-driven domain wall motions . It shows a nonlinear dependence of the wall speed on the current density which agrees with the experiments in [1].

Index Terms—Spin dynamics, magnetization dynamics, spin-magnetization coupling, domain wall motion.

I. INTRODUCTION

UNDERSTANDING the spin-magnetization coupling in ferromagnetic materials is crucial for the active control of domain-wall motions [2], [3], [4] and magnetization reversals in magnetic multilayers [5], which are the core techniques for magnetoresistance random access memories, and race-track memories [6]. Spin dynamics include spin polarization, spin transport and diffusion within ferromagnets, and spin-magnetization interactions [7], [8], [6]. In the spin-magnetization coupling, the spin angular momentum is transferred to magnetization dynamics by a mechanism known as spin-transfer torque (STT). This has been observed in experiments on a variety of magnetic materials, including metals (*e.g.*, Fe, Co, Ni, and their alloys [7], [6]) and semiconductors (*e.g.*, diamond and organic semiconductors [9], [10], [11]).

The studies on STT were initiated by the seminal works of Slonczewski [12] and Berger [13], and recent progress can be classified into two categories based on the forms of STT in model equations: In the first kind, STT is written explicitly in terms of the magnetization and its derivatives [14], [15], [16], [17]; in the second kind, STT is treated as a variable that couples spin and magnetization dynamics [18], [19], [20]. The spin-magnetization coupled system can be reduced to magnetization dynamics only but with an extra magnetization-dependent torque, under the assumption of the spatial homogeneity of the spin current [14].

For models of spin dynamics, there have been a few attempts to derive macroscopic models from a microscopic level [20], [16], [17]. For models of magnetization dynamics, only [17] contains additional torques derived from a microscopic level. A kinetic model for spin dynamics was derived in [20], but did not explain the linear response theory [18] in a straightforward

way. This motivates us to study the connection of physical models of spin dynamics at different scales by deriving mean-field models for spin dynamics starting from a microscopic description. We also couple the mean-field models to magnetization dynamics given by the Landau-Lifshitz-Gilbert (LLG) equation [21], [22] to further study the interaction of spin and magnetization. The method introduced here is systematic, and can be generalized for deriving mean-field models of the spin-orbit coupling in magnetic bilayers (*e.g.*, Co/Pt, [23], [24], [25]) by including the Rashba spin-orbit coupling term [26].

In Section II, we describe the spin dynamics by connecting a Schrödinger equation of the spinor form to kinetic equations by the Wigner transform. A mean-field model is further derived by carrying out a moment closure approximation on the kinetic equations with Bloch collision terms. Under the quasi-static approximation on charge and spin currents, the mean-field model leads to the Zhang-Levy-Fert's model proposed in [18] but with an extra non-isotropic diffusion term, which vanishes and recovers the Zhang-Levy-Fert's model in the weak spin-magnetization coupling regime. The importance of this diffusion term is discussed in Section III in the context of current-driven domain wall motions with fully three-dimensional numerical simulations. We make conclusive remarks and discuss the generalization to the spin-orbit coupling in Section IV.

II. SPIN DYNAMICS AT DIFFERENT PHYSICAL SCALES

Our starting point is the dynamics of a spinor in a one-body approximation given by the Schrödinger equation

$$i\hbar\frac{\partial}{\partial t}\boldsymbol{\psi}(\boldsymbol{x},t) = \mathcal{H}(\boldsymbol{x},t)\boldsymbol{\psi}(\boldsymbol{x},t), \tag{1}$$

where $\boldsymbol{\psi} = (\psi_+, \psi_-)^T$ is the spinor, and the effective Hamiltonian is of the form [16]

$$\mathcal{H}(\boldsymbol{x}, t) = \left(-\frac{\hbar^2}{2m}\nabla_{\boldsymbol{x}}^2 + V(\boldsymbol{x})\right) - \frac{c}{2}\hat{\boldsymbol{\sigma}} \cdot \boldsymbol{m}(\boldsymbol{x}, t), \quad (2)$$

where c is the spin-magnetization coupling constant, $\boldsymbol{m}$ is the magnetization, and $\hat{\boldsymbol{\sigma}}$ are Pauli matrices. Here we use c for the spin-magnetization coupling constant to distinguish it from J_{sd} typically saved for the $s-d$ exchange coupling constant. The magnitude of J_{sd} is around $0.1 \sim 1$ eV in the literature; see [14] for example, while the magnitude of c is very difficult to be measured in experiments [1]. In Section III, we shall discuss how the spin-magnetization coupling constant c can be extracted from one set of experimental measurements, and produce consistent results with another set of experimental measurements.

The kinetic description of spinor dynamics is provided by the following Wigner function $W(\boldsymbol{x}, \boldsymbol{v}, t)$:

$$W = (\frac{m}{2\pi\hbar})^3 \int_{\mathbb{R}^3} \boldsymbol{\psi}(\boldsymbol{x} - \frac{\boldsymbol{y}}{2}, t) \otimes \boldsymbol{\psi}^*(\boldsymbol{x} + \frac{\boldsymbol{y}}{2}, t)e^{i\frac{m}{\hbar}\boldsymbol{v}\cdot\boldsymbol{y}}\,d\boldsymbol{y},$$

whose dynamics follow the Boltzmann equation

$$\partial_t W + \boldsymbol{v} \cdot \nabla_{\boldsymbol{x}}W - \frac{e}{m}\boldsymbol{E}\cdot\nabla_{\boldsymbol{v}}W - \frac{ic[\hat{\boldsymbol{\sigma}}\cdot\boldsymbol{m}, W]}{2\hbar}$$
$$= -\left(\frac{\partial W}{\partial t}\right)_{\text{colli}}, \quad (3)$$

where the electric field $\boldsymbol{E} = \nabla V/e$, and the collision term $\left(\frac{\partial W}{\partial t}\right)_{\text{colli}} = \frac{W - \overline{W}}{\tau} + \frac{2}{\tau_{\text{sf}}}(\overline{W} - \frac{I}{2}\text{Tr}\overline{W})$ is in s-wave form [20]. Here τ and τ_{sf} are the characteristic time scales of momentum relaxation and spin flipping, $\overline{W} = \frac{1}{4\pi}\int d\Omega_{\boldsymbol{v}}W(\boldsymbol{x}, \boldsymbol{v}, t)$ is the angular average over the $\boldsymbol{v}$ space, and Tr represents the trace operator over the spin space. Note that τ is much smaller than τ_{sf} [27], [28], which implies electron collision happens much faster than spin flipping. Typically, τ is of 1fs and τ_{sf} is of 1ps.

$W(\boldsymbol{x}, \boldsymbol{v}, t)$ is connected to the macroscopic quantities via its moments: Charge density $n(\boldsymbol{x}, t) = \int_{\mathbb{R}^3}\text{Tr}(W)\,d\boldsymbol{v}$, charge current $\boldsymbol{j}_n(\boldsymbol{x}, t) = \int_{\mathbb{R}^3}\boldsymbol{v}\text{Tr}(W)\,d\boldsymbol{v}$, spin density $\boldsymbol{s}(\boldsymbol{x}, t) = \int_{\mathbb{R}^3}\text{Tr}(\hat{\boldsymbol{\sigma}}W)\,d\boldsymbol{v}$, and spin current $J_{\boldsymbol{s}}(\boldsymbol{x}, t) = \int_{\mathbb{R}^3}\boldsymbol{v}\otimes\text{Tr}(\hat{\boldsymbol{\sigma}}W)\,d\boldsymbol{v}$.

Decompose $W = wI + \hat{\boldsymbol{\sigma}}\cdot\boldsymbol{\eta}$, where w is spin-independent and $\boldsymbol{\eta}$ is spin-dependent. We propose the following closure conditions originally used in a similar form in [29] for the study of chemotaxis which approximate w and $\boldsymbol{\eta}$ by linearly combined macroscopic quantities $\{n(\boldsymbol{x}, t), n_1(\boldsymbol{x}, t), \boldsymbol{m}, \boldsymbol{m}_1(\boldsymbol{x}, t)\}$ with spanning coefficients $\{\gamma_j, \gamma'_j\}_{j=0}^3$

$$w(\boldsymbol{x}, \boldsymbol{v}, t) = f(\boldsymbol{v})\{\gamma_0 n(\boldsymbol{x}, t) + \gamma_1 \boldsymbol{m}\cdot\boldsymbol{s}(\boldsymbol{x}, t)$$
$$+ \boldsymbol{\gamma}_2\cdot\boldsymbol{v}n_1(\boldsymbol{x}, t) + \gamma_3\boldsymbol{v}\cdot\boldsymbol{m}_1(\boldsymbol{x}, t)\},$$

$$\boldsymbol{\eta}(\boldsymbol{x}, \boldsymbol{v}, t) = g(\boldsymbol{v})\{\gamma'_0\boldsymbol{m}n(\boldsymbol{x}, t) + \gamma'_1\boldsymbol{s}(\boldsymbol{x}, t)$$
$$+ \gamma'_2\boldsymbol{v}n_1(\boldsymbol{x}, t) + \gamma'_3\boldsymbol{v}(\boldsymbol{m}\cdot\boldsymbol{m}_1(\boldsymbol{x}, t))\},$$

where f and g are normalized Gaussian functions to make w and $\boldsymbol{\eta}$ decay at infinity of momentum space. Here $n_1(\boldsymbol{x}, t)$

[1]Eiji Saitoh (private communication).

and $\boldsymbol{m}_1(\boldsymbol{x}, t)$ are next-order corrections to charge and spin densities, respectively. They can be specified only when the detailed information of Wigner function is available. With these closure assumptions and some calculus, we obtain a closed mean-field description for the charge and spin dynamics

$$\partial_t n + \nabla_{\boldsymbol{x}}\boldsymbol{j}_n = 0, \quad (4)$$

$$\partial_t\boldsymbol{j}_n + \gamma_0\overline{v^2}\nabla_{\boldsymbol{x}}n + \gamma_1\overline{v^2}\nabla_{\boldsymbol{x}}\boldsymbol{s}\boldsymbol{m} + \frac{e}{m}\boldsymbol{E}n = -\frac{\boldsymbol{j}_n}{\tau}, \quad (5)$$

$$\partial_t\boldsymbol{s} + \nabla_{\boldsymbol{x}}J_{\boldsymbol{s}} + \frac{c}{\hbar}\boldsymbol{m}\times\boldsymbol{s} = -\frac{\boldsymbol{s}}{\tau_{\text{sf}}}, \quad (6)$$

$$\partial_t J_{\boldsymbol{s}} + \gamma'_0\overline{v^2}\nabla_{\boldsymbol{x}}n\otimes\boldsymbol{m} + \gamma'_1\overline{v^2}\nabla_{\boldsymbol{x}}\boldsymbol{s} + \frac{e}{m}\boldsymbol{E}\otimes\boldsymbol{s}$$
$$+ \frac{c}{\hbar}\varepsilon_{jkl}\boldsymbol{m}_k(J_{\boldsymbol{s}})_{il} = -\frac{J_{\boldsymbol{s}}}{\tau}. \quad (7)$$

Note that, under the proposed closure approximations, $\{n(\boldsymbol{x}, t), \boldsymbol{j}_n(\boldsymbol{x}, t)\}$ and $\{\boldsymbol{s}(\boldsymbol{x}, t), J_{\boldsymbol{s}}(\boldsymbol{x}, t)\}$ are coupled, *i.e.*, the dynamics of charge density and charge current is affected by the dynamics of spin density and spin current, and vice versa. This is, however, different from the decoupled system obtained in [20], where the authors assumed the dependence of $w(\boldsymbol{x}, \boldsymbol{v}, t)$ only on $n(\boldsymbol{x}, t)$ and $n_1(\boldsymbol{x}, t)$ and $\boldsymbol{\eta}(\boldsymbol{x}, \boldsymbol{v}, t)$ only on $\boldsymbol{m}$ and $\boldsymbol{s}(\boldsymbol{x}, t)$, respectively. In the presence of the spin-magnetization interaction, our model seems more physical.

In order to further get drift-diffusion equations for spin dynamics, we shall study the long-time behavior of the above coupled system (4)-(7). In the diffusive regime, charge current and spin current shall saturate to equilibrium charge current and equilibrium spin current, respectively. We thus drop their temporal derivatives. Furthermore, the spatial variation of charge density is assumed to be very small and can be ignored [18]. The diffusion equation for spin dynamics reads as [2]

$$\partial_t\boldsymbol{s} = -\nabla_{\boldsymbol{x}}\cdot J_{\boldsymbol{s}} - \frac{\boldsymbol{s}}{\tau_{\text{sf}}} - \frac{\boldsymbol{s}\times\boldsymbol{m}}{\tau_c}, \quad (8)$$

$$J_{\boldsymbol{s}}\boldsymbol{A} = \frac{\beta\mu_{\text{B}}}{e}\boldsymbol{j}_n\otimes\boldsymbol{m} - D[\nabla\boldsymbol{s} - \beta\beta'(\nabla\boldsymbol{s}\cdot\boldsymbol{m})\otimes\boldsymbol{m}], \quad (9)$$

$$\boldsymbol{A} = \begin{pmatrix} 1 & \frac{\tau}{\tau_c}m_3 & -\frac{\tau}{\tau_c}m_2 \\ -\frac{\tau}{\tau_c}m_3 & 1 & \frac{\tau}{\tau_c}m_1 \\ \frac{\tau}{\tau_c}m_2 & -\frac{\tau}{\tau_c}m_1 & 1 \end{pmatrix}, \quad (10)$$

where $\tau_c = \hbar/c$ is the characteristic time scale of the spin-magnetization coupling, D is the diffusivity, β is the spin polarization parameter for conductivity, and β' is the other spin polarization parameter for diffusivity.

In general, $\boldsymbol{A}$ has eigenvalues 1, $1 \pm \frac{\tau}{\tau_c}i$ and $\det\boldsymbol{A} = 1 + (\frac{\tau}{\tau_c})^2$. τ_c depends on the strength of the spin-magnetization coupling. There are two main consequences of this: (1) Purely imaginary contributions in the eigenvalues of $\boldsymbol{A}$, which contribute to energy dispersion in the coupled system; (2) $\det\boldsymbol{A}$ is always ≥ 1, which contributes to energy dissipation. From a mathematical viewpoint, it is also worth mentioning that the appearance of $\boldsymbol{A}$ is independent of the closure technique.

In [18], the spin-magnetization coupling only appears in the LLG equation (11) in the framework of linear response theory.

[2]The factor 2 was explicitly used in [18], while here is included in the definition of macroscopic quantities. Terms with γ_0 and γ'_0 vanish in (5) and (7). $\boldsymbol{E}$ can be solved in (5) and then substituted into (7), which results (9) and (10) with $D = \gamma'_1\overline{v^2}\tau$, $\beta = e\boldsymbol{s}/(\mu_{\text{B}}n\boldsymbol{m})$, and $\beta' = \mu_{\text{B}}\gamma_1/(e\gamma'_1)$.

In our model, it appears in both LLG equation (11) and spin diffusion (8)-(10), which seems more natural. In the regime $\tau_c \gg \tau$, $\boldsymbol{A}$ approaches the identity matrix, the moment system in the diffusive regime recovers the diffusion model derived from the linear response theory [18], which corresponds to the limit of weak spin-magnetization coupling. However, beyond that, these two models are different. When the coupling is not weak, these effects can be significant, as illustrated in the current-driven magnetization reversal simulations presented in [30].

The dynamics of the magnetization, in the presence of a spin-transfer torque, are described by the LLG equation [21], [22],

$$\frac{\partial \boldsymbol{m}}{\partial t} = -\gamma \boldsymbol{m} \times (\boldsymbol{H}_\mathrm{e} + c\boldsymbol{s}) + \alpha \boldsymbol{m} \times \frac{\partial \boldsymbol{m}}{\partial t} \quad (11)$$

with the normalized magnetization $\boldsymbol{m}(\boldsymbol{x}, t) = (m_1(\boldsymbol{x}, t), m_2(\boldsymbol{x}, t), m_3(\boldsymbol{x}, t))^T$ defined over the uniaxial ferromagnetic material

In a uniaxial material, the effective field $\boldsymbol{H}_\mathrm{e}$ reads as

$$\boldsymbol{H}_\mathrm{e} = -\frac{2K_\mathrm{u}}{M_\mathrm{s}}(m_2\boldsymbol{e}_2 + m_3\boldsymbol{e}_3) + \frac{2C_\mathrm{ex}}{M_\mathrm{s}}\Delta\boldsymbol{m} + \mu_0(\boldsymbol{H}_\mathrm{s} + \boldsymbol{H}_0). \quad (12)$$

$\boldsymbol{e}_2 = (0, 1, 0)$, $\boldsymbol{e}_3 = (0, 0, 1)$, and $\mu_0 = 4\pi \times 10^{-7}$ N/A^2 is the permeability of vacuum. K_u and C_ex are materials constants, and M_s is the saturation magnetization which is also material-dependent. For physical constants characteristic of the permalloy, $K_\mathrm{u} = 5.0 \times 10^2$ J/m^3, $C_\mathrm{ex} = 1.3 \times 10^{-11}$ J/m, and $M_\mathrm{s} = 8.0 \times 10^5$ A/m. $\boldsymbol{H}_0$ is the externally applied magnetic field and $\boldsymbol{H}_\mathrm{s}$ is the stray field, given by $\boldsymbol{H}_\mathrm{s} = -\nabla u$, where

$$u(\boldsymbol{x}) = \int_\Omega \nabla N(\boldsymbol{x} - \boldsymbol{y}) \cdot \boldsymbol{m}(\boldsymbol{y}) \, \mathrm{d}\boldsymbol{y}, \quad (13)$$

where $N(\boldsymbol{x}) = -1/(4\pi|\boldsymbol{x}|)$ is the Newtonian potential.

III. DOMAIN WALL DYNAMICS

Experimental studies on domain wall dynamics have been carried out on many materials and devices [2], [31], [1], [3], [4], in which the spin-magnetization interaction [14], [15], the Rashba spin-orbit coupling [32], and the Dzyaloshinskii-Moriya interaction [33], [34] play important roles. Since only the spin-magnetization interaction is considered in our work, to make an unambiguous comparison between theory and experiment, we consider the ferromagnetic device used in [31], [1] where Permalloy ($Ni_{81}Fe_{19}$) is considered under applied currents. A vortex domain wall structure is initialized in the sample with dimensions 2.5 μm $\times$ 240 nm $\times$ 10 nm. Fig. 1(a) shows the initial domain wall structure, which is consistent with the image observed by magnetic force microscopy [31]. Fig. 1(b) and 1(c) are detailed configurations of the vortex wall and the centered vortex after zooming in, respectively.

To simulate the domain wall dynamics, we discretize the sample with grid sizes $\Delta x = \Delta y = \Delta z = 2.5$ nm, and solve the spin dynamics (8) using a time-splitting scheme [35], [30] and the magnetization dynamics (11) using the Gauss-Seidel Projection Method [36]. It is observed that the domain wall dynamics cannot be resolved if 5 nm grid size is used. Temporal stepsizes for spin dynamics and magnetization dynamics are 1 fs and 0.1 ps, respectively. Qualitatively, the
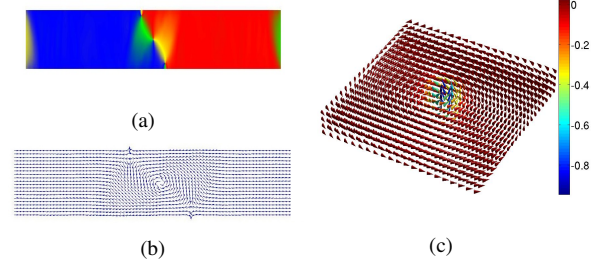
Fig. 1. Simulated domain wall structures with dimensions of illustrations (unit: nm) : (a) $[0, 2500] \times [0, 240] \times \{z = 5\}$; (b) $[700, 1800] \times [0, 240] \times \{z = 5\}$; (c) $[1200, 1300] \times [28, 68] \times [0, 10]$. 2500 nm is used for later simulations since it is large enough to avoid the interaction between the vortex wall and boundaries in the x direction. (a) Initialized vortex wall colored by the angle between $m_1(\boldsymbol{x}, t)$ and $m_2(\boldsymbol{x}, t)$, consistent with the image obtained by the magnetic force microscopy [31]. (b) Zooming in the vortex wall with arrows specified by $m_1(\boldsymbol{x}, t)$ and $m_2(\boldsymbol{x}, t)$. (c) Cone plot of the centered vortex in 3D with directions specified by $\boldsymbol{m}(\boldsymbol{x}, t)$. Thin film structure of the device results in uniform magnetization in the z direction.
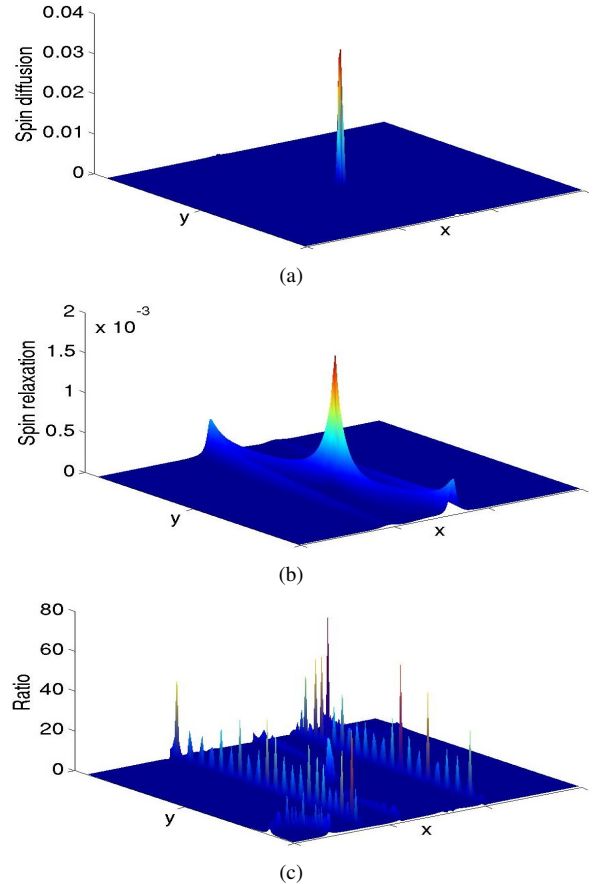
Fig. 2. Simulated spin diffusion and spin relaxation with dimensions of illustrations (unit: nm) $[700, 1800] \times [0, 240] \times \{z = 5\}$, which is the same as that in Fig. 1(b). (a) $|\nabla \cdot (D(\nabla \boldsymbol{s})\boldsymbol{A}^{-1})|$ (ps^{-1}). The centered peak corresponds to the core of the vortex in Fig. 2(c). (b) $|\boldsymbol{s}/\tau_\mathrm{sf}|$ (ps^{-1}). Inhomogeneity happens around the core of the vortex (Fig. 2(c) and 2(b)). (c) $|\nabla \cdot (D(\nabla \boldsymbol{s})\boldsymbol{A}^{-1})|/(|\boldsymbol{s}/\tau_\mathrm{sf}|)$ (dimensionless). Averaging of $|\nabla \cdot (D(\nabla \boldsymbol{s})\boldsymbol{A}^{-1})|/(|\boldsymbol{s}/\tau_\mathrm{sf}|)$ over space produces a ratio around 0.25, which implies spin diffusion cannot be ignored. Peaks in the core of the vortex wall further implies the importance of the geometric information of the wall structure.

wall moves in the opposite direction of the applied current, consistent with the experimental result.

For Permalloy, the damping parameter α is around 0.01, as determined by first-principle calculations [37]. However, the coupling constant c is unfortunately not available from the literature. For the same material, it has been measured in [1] that the wall velocity is 3 m/s when the applied current $\boldsymbol{j}_n = 7.1 \times 10^{11}$ A/m^2. A generic way of estimating c is to use experimental results to study the relationship between the coupling constant c and the domain wall velocity. A linear dependence is observed in Fig. 3(a). Fig. 3(b) shows how the wall velocity changes as time evolves. The wall structure is initially self-adjusted, then moves in the opposite direction of the applied current. Its velocity saturates after 17 ns, which is close to the raise time of the current pulse 15 ns [31]. Limited by the spatial resolution, the instantaneous velocity is not smooth, but it is adequate to resolve the domain wall dynamics. Wall displacements and velocities in experiments are measured over micro seconds, which suggests saturated velocities in simulations should be used for comparison. A careful study illustrates that the coupling constant c necessary to generate the wall velocity 3.2 m/s as in the experiment is around 2×10^{-4} eV. Other walls, such as the transverse wall and the head-to-head wall, have also been examined, and the wall velocities were found to be around 3 m/s.

It is mentioned in [19] that the magnitude of c is around $0.1 \sim 1$ eV. Following Walker's prescription of the domain wall used in [14], the estimated velocity of a Néel wall was around 3 m/s when $c = 5 \times 10^{-2}$ eV. Using the same procedure for the coupling constant in our model, we apply the Gauss-Seidel Projection Method for the fully three-dimensional simulation of Equation (11) in [14] for the vortex wall; see Fig. 3(d). The simulated wall velocity is around 3 m/s for a slightly different $c = 5.5 \times 10^{-2}$ eV. Other walls, such as the transverse wall and the head-to-head wall, are also examined with wall velocities around 2.8 m/s. This suggests that the domain wall velocity is insensitive to the discrepancy in the domain wall structure. It is worth mentioning that if additionally the injection geometry and torque origins are changed, a larger difference has been observed [38].

It is quite surprising that the coupling constant in our model (8)-(11) is over two orders of magnitude smaller than that in the Zhang-Li's model [14] in order to achieve the quantitative agreement with experiments on the domain wall velocity. We believe the discrepancy is mainly due to the fact that the spin diffusion term $\nabla \cdot (D \nabla \boldsymbol{s})$ is neglected in the Zhang-Li's model. Our simulations show that, compared with the spin relaxation term $\boldsymbol{s}/\tau_{\mathrm{sf}}$, the spin diffusion term is not negligible. Spatially averaged $|\nabla \cdot (D(\nabla \boldsymbol{s}) \boldsymbol{A}^{-1})|/(|\boldsymbol{s}/\tau_{\mathrm{sf}}|)$ is around 0.25, which is not small enough to be ignored. Moreover, in the core of the vortex wall, both spin diffusion and spin relaxation terms have increments and peaks (Fig. 2). The ratio between these two terms peaks with magnitudes over 50, showing the importance of the geometric information of the vortex wall. Studies on other wall structures also support that the spin diffusion term is not negligible in the core region of wall structures.

To further examine our model, we shall fix $c = 2 \times 10^{-4}$ eV in our model and $c = 5.5 \times 10^{-2}$ eV in Zhang-Li's model,
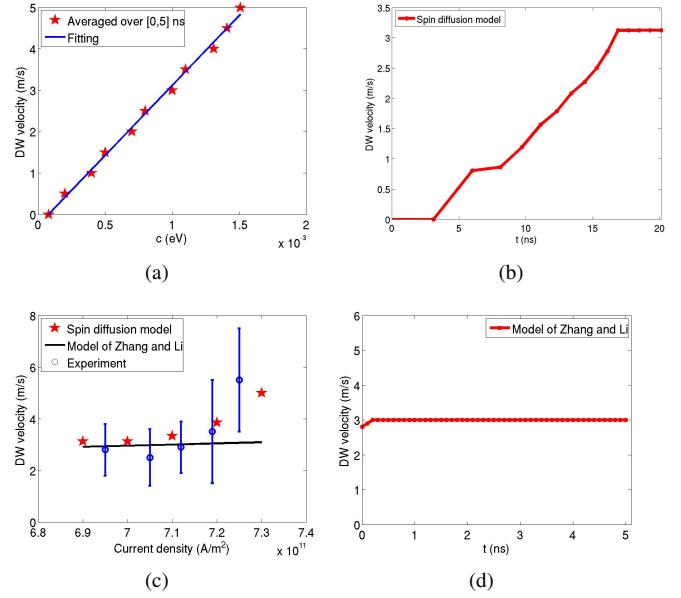
Fig. 3. Simulated domain wall velocities: (a)-(c): spin dynamics (8) coupled to the LLG equation; (d) The LLG equation with additional torques [14]. (a) Averaged domain wall velocity over $[0,5]$ ns as a function of the coupling constant c. A linear dependence of the velocity on c is observed. (b) Instantaneous domain wall velocity as a function of time, which saturates around 3 m/s. The wall velocity saturates around 17 ns, which is close to the raise time of current pulses 15 ns in experiments [31]. (c) Saturated domain wall velocities as a function of the applied current density. A nonlinear dependence is observed in our model, which agrees nicely with experiments [1], while a linear dependence is obtained in Zhang-Li's model. (d) Instantaneous domain wall velocity as a function of time, which stabilizes around 3 m/s. Compared with Fig. 3(b), magnetization dynamics saturates quickly due to the lack of spin dynamics.

and simulate the domain wall velocity as a function of the applied current density. A nonlinear dependence of the wall velocity on the applied current density is observed in [1]. Fig. 3(c) plots simulated wall velocities in terms of the applied current density in our model and Zhang-Li's model. Result in our model matches the experimental result quite well with a nonlinear dependence, while only a linear dependence in Zhang-Li's model is observed. It is clear that the inclusion of the spin diffusion in the present work is responsible for the nonlinear dependence of the wall velocity on the applied current density. However, the fitting is not perfect, particularly for higher current densities in Fig. 3(c). A possible reason is that the presence of applied current introduces the heating effect [1], which may further produce an inhomogeneous temperature distribution in the sample. It has been reported that the thermally-driven domain wall velocity depends on the temperature gradient both theoretically [39] and experimentally [40]. The heating effect therefore may also contribute to the domain wall motion.

While there is no experimental data for the spin-magnetization coupling constant of the considered material, there are measurements on the s-d coupling constant of various materials. For example, for Supermalloy (Ni$_{75}$Fe$_{20}$Mo$_5$), the measured coupling constant is around 0.1 eV [41], which actually describes the coupling between s and d electrons in the ferromagnet and used in [14]. However, to what extent

the coupling constant of the exchange interaction between s and d electrons can well represent the spin-magnetization coupling constant is unclear, especially in the presence of applied currents. Extrinsic electrons due to applied currents are farther away from d electrons of the material compared to the native s electrons of the material, and therefore a smaller coupling constant is expected. Actually, it is very difficult to measure the coupling constant for the material considered here [3]. We expect the coupling between the spin of the itinerant electrons and the magnetization to be weaker. It is therefore not necessarily clear that this experimental value is the appropriate one for the system at hand, and due to the lack of a strong theoretical argument to choose the coupling constant, we fit the coupling constants in our model and Zhang-Li's model.

We would also like to point out that in the weak coupling regime considered, our model recovers the model developed by Shpiro, Zhang, and Fert [19], and therefore the wall velocity we obtain is consistent with the wall velocity obtained with their model. The model introduced by Zhang and Li [14] is derived from the model developed by Shpiro, Zhang, and Fert, and neglects spin diffusion under the assumption that the variation of s is small. We believe this is the main reason for the discrepancy in the wall velocity, and the coupling constant used: s varies considerably in the vicinity of the wall (Fig. 2), and therefore that term cannot be neglected. Moreover, the inclusion of the spin diffusion is responsible for the nonlinear dependence of the wall velocity on the applied current density.

IV. Conclusion and Discussion

We present a new mean-field model for the dynamics of the spin-magnetization coupling in ferromagnetic materials. The coupling introduces off-diagonal terms of (10) in the spin dynamics whose formula are independent of closure assumptions and explicitly reveal the coupling strength. In the weak spin-magnetization coupling regime ($\tau/\tau_c \ll 1$), the model recovers the Zhang-Levy-Fert's model [18]. Nontrivial features of the model were studied for current-driven domain wall motions via fully three-dimensional numerical simulations.

Recent developments for current-driven magnetization dynamics include the generalization of LLG equation [42], the generalization of the drift-diffusion equation for spin dynamics [43], and the semiclassical modeling of spin dynamics [44], [25]. In [42], the LLG equation is generalized by explicitly including a 3×3 differential damping tensor that represents the effect of conduction electrons in the magnetization dynamics introduced using Ohm's law for electron and spin currents. In [43], the drift-diffusion equation for spin dynamics is generalized by using a generalized Ohm's law for electron and spin currents. Both approaches rely on the constitutive relations at the macroscopic scale. In [44], [25], the authors use a semiclassical spin dynamics approach, and tune the collision term in the Boltzmann equation in order to match the results obtained by the LLG equation with an additional, predetermined spin torque, as opposed to deriving the corresponding shape of the spin torque from a predetermined

microscopic equation. From a modeling viewpoint, we stress that our approach is systematic, and produces a connection from quantum mechanics (1), to the Boltzmann equation (3), and then to the moment system (4)-(7), and finally to the drift-diffusion equation (8)-(9).

Although only the drift-diffusion equation has been examined carefully, other models, such as the moment system and the Boltzmann equation, could be helpful to understand experimental results in other scenarios. For example, femtosecond spin dynamics in experiments [45] cannot be well described by the drift-diffusion equation (8)-(9), and the moment system (4)-(7) shall play an important role in this case.

Moreover, our approach can be generalized to the case of the spin-orbit coupling. Preliminary results show that the corresponding Boltzmann equation has a new term, which is absent in the Boltzmann equation in the current work and [25], [44]. How this new term affects macroscopic equations and what is the connection of this new term to the additional torque due to the spin-orbit coupling in the LLG equation is currently being considered by the authors and will appear elsewhere.

References

[1] A. Yamaguchi, T. Ono, S. Nasu, K. Miyake, K. Mibu, and T. Shinjo, "Erratum: Real-space observation of current-driven domain wall motion in submicron magnetic wires [phys. rev. lett. 92, 077205 (2004)]," *Phys. Rev. Lett.*, vol. 96, p. 179904, May 2006.

[2] T. Ono, H. Miyajima, K. Shigeto, K. Mibu, N. Hosoito, and T. Shinjo, "Propagation of a magnetic domain wall in a submicrometer magnetic wire," *Science*, vol. 284, no. 5413, pp. 468–470, 1999.

[3] I. M. Miron, T. Moore, H. Szambolics, L. D. Buda-Prejbeanu, S. Auffret, B. Rodmacq, S. Pizzini, J. Vogel, M. Bonfim, A. Schuhl, and G. Gaudin, "Fast current-induced domain-wall motion controlled by the Rashba effect," *Nat. Mater.*, vol. 10, pp. 419–423, 2011.

[4] S. Emori, U. Bauer, S.-M. Ahn, E. Martinez, and G. S. D. Beach, "Current-driven dynamics of chiral ferromagnetic domain walls," *Nat. Mater.*, vol. 12, pp. 611–616, 2013.

[5] M. N. Baibich, J. M. Broto, A. Fert, F. N. Van Dau, F. Petroff, P. Etienne, G. Creuzet, A. Friederich, and J. Chazelas, "Giant magnetoresistance of (001)Fe/(001)Cr magnetic superlattices," *Phys. Rev. Lett.*, vol. 61, pp. 2472–2475, Nov 1988.

[6] A. Brataas, A. D. Kent, and H. Ohno, "Current-induced torques in magnetic materials," *Nat. Mater.*, vol. 11, pp. 372–381, 2012.

[7] I. Žutić, J. Fabian, and S. Das Sarma, "Spintronics: Fundamentals and applications," *Rev. Mod. Phys.*, vol. 76, pp. 323–410, Apr 2004.

[8] D. Ralph and M. Stiles, "Spin transfer torques," *J. Magn. Magn. Mater.*, vol. 320, no. 7, pp. 1190 – 1216, 2008.

[9] R. Hanson, F. M. Mendoza, R. J. Epstein, and D. D. Awschalom, "Polarization and readout of coupled single spins in diamond," *Phys. Rev. Lett.*, vol. 97, p. 087601, Aug 2006.

[10] S. Sanvito, "Organic spintronics: Filtering spins with molecules," *Nat. Mater.*, vol. 10, pp. 484–485, 2011.

[11] T. Dietl and H. Ohno, "Dilute ferromagnetic semiconductors: Physics and spintronic structures," *Rev. Mod. Phys.*, vol. 86, pp. 187–251, Mar 2014.

[12] J. Slonczewski, "Current-driven excitation of magnetic multilayers," *J. Magn. Magn. Mat.*, vol. 159, pp. L1–L7, 1996.

---

[3] Eiji Saitoh (private communication).

[13] L. Berger, "Emission of spin waves by a magnetic multilayer traversed by a current," *Phys. Rev. B*, vol. 54, pp. 9353–9358, 1996.

[14] S. Zhang and Z. Li, "Roles of nonequilibrium conduction electrons on the magnetization dynamics of ferromagnets," *Phys. Rev. Lett.*, vol. 93, p. 127204, Sep 2004.

[15] G. Tatara and H. Kohno, "Theory of current-driven domain wall motion: Spin transfer versus momentum transfer," *Phys. Rev. Lett.*, vol. 92, p. 086601, Feb 2004.

[16] F. Piéchon and A. Thiaville, "Spin transfer torque in continuous textures: Semiclassical Boltzmann approach," *Phys. Rev. B*, vol. 75, p. 174414, May 2007.

[17] R. Cheng and Q. Niu, "Microscopic derivation of spin-transfer torque in ferromagnets," *Phys. Rev. B*, vol. 88, p. 024422, Jul 2013.

[18] S. Zhang, P. M. Levy, and A. Fert, "Mechanisms of spin-polarized current-driven magnetization switching," *Phys. Rev. Lett.*, vol. 88, p. 236601, May 2002.

[19] A. Shpiro, P. M. Levy, and S. Zhang, "Self-consistent treatment of nonequilibrium spin torques in magnetic multilayers," *Phys. Rev. B*, vol. 67, p. 104430, Mar 2003.

[20] Y. Qi and S. Zhang, "Spin diffusion at finite electric and magnetic fields," *Phys. Rev. B*, vol. 67, p. 052407, Feb 2003.

[21] L. Landau and E. Lifshitz, "On the theory of the dispersion of magnetic permeability in ferromagnetic bodies," *Phys. Z. Sowj.*, vol. 8, pp. 153–169, 1935.

[22] T. Gilbert, *Phys. Rev.*, vol. 100, p. 1243, 1955.

[23] S. Emori, U. Bauer, S.-M. Ahn, E. Martinez, and G. Beach, "Current-driven dynamics of chiral ferromagnetic domain walls," *Nature Materials*, vol. 12, pp. 611–616, 2013.

[24] K. Garello, I. M. Miron, C. O. Avci, F. Freimuth, Y. Mokrousov, S. Blügel, S. Auffret, O. Boulle, G. Gaudin, and P. Gambardella, "Symmetry and magnitude of spin-orbit torques in ferromagnetic heterostructures," *Nature Nanotechnology*, vol. 8, pp. 587–593, 2013.

[25] P. M. Haney, H.-W. Lee, K.-J. Lee, A. Manchon, and M. D. Stiles, "Current induced torques and interfacial spin-orbit coupling: Semiclassical modeling," *Phys. Rev. B*, vol. 87, p. 174411, 2013.

[26] Y. A. Bychkov and E. I. Rashba, "Properties of a 2D electron gas with lifted spectral degeneracy," *JETP Lett.*, vol. 39, pp. 78–81, 1984.

[27] G. D. Gaspari, "Bloch equation for conduction-electron spin resonance," *Phys. Rev.*, vol. 151, pp. 215–219, Nov 1966.

[28] J. I. Kaplan, "Diffusion constant in the effective Bloch equation for ferromagnetic resonance in metals," *Phys. Rev.*, vol. 143, pp. 351–352, Mar 1966.

[29] T. Hillen, "Hyperbolic models for chemosensitive movement," *Math. Models and Methods in Appl. Sci.*, vol. 12, pp. 1007–1034, 2002.

[30] J. Chen, C. J. García-Cervera, and X. Yang, "A mean-field model of spin dynamics in multilayered ferromagnetic media," *submitted*, 2014.

[31] A. Yamaguchi, T. Ono, S. Nasu, K. Miyake, K. Mibu, and T. Shinjo, "Real-space observation of current-driven domain wall motion in submicron magnetic wires," *Phys. Rev. Lett.*, vol. 92, p. 077205, Feb 2004.

[32] K.-W. Kim, J.-H. Moon, K.-J. Lee, and H.-W. Lee, "Prediction of giant spin motive force due to rashba spin-orbit coupling," *Phys. Rev. Lett.*, vol. 108, p. 217202, May 2012.

[33] I. Dzyaloshinsky, "A thermodynamic theory of weak ferromagnetism of antiferromagnetics," *J. Phys. Chem. Solids*, vol. 4, no. 4, pp. 241 – 255, 1958.

[34] T. Moriya, "Anisotropic superexchange interaction and weak ferromagnetism," *Phys. Rev.*, vol. 120, pp. 91–98, Oct 1960.

[35] C. J. García-Cervera and X.-P. Wang, "Spin-polarized currents in ferromagnetic multilayers," *J. Comput. Phys.*, vol. 224, no. 2, pp. 699–711, 2007.

[36] X.-P. Wang, C. J. García-Cervera, and W. E, "A Gauss-Seidel projection method for the Landau-Lifshitz equation," *J. Comp. Phys.*, vol. 171, pp. 357–372, 2001.

[37] A. A. Starikov, P. J. Kelly, A. Brataas, Y. Tserkovnyak, and G. E. W. Bauer, "Unified first-principles study of gilbert damping, spin-flip diffusion, and resistivity in transition metal alloys," *Phys. Rev. Lett.*, vol. 105, p. 236601, Dec 2010.

[38] A. V. Khvalkovskiy, V. Cros, D. Apalkov, V. Nikitin, M. Krounbi, K. A. Zvezdin, A. Anane, J. Grollier, and A. Fert, "Matching domain-wall configuration and spin-orbit torques for efficient domain-wall motion," *Phys. Rev. B*, vol. 87, p. 020402, Jan 2013.

[39] J. Xiao, G. E. W. Bauer, K.-c. Uchida, E. Saitoh, and S. Maekawa, "Theory of magnon-driven spin seebeck effect," *Phys. Rev. B*, vol. 81, p. 214418, Jun 2010. [Online]. Available: http://link.aps.org/doi/10.1103/PhysRevB.81.214418

[40] W. Jiang, P. Upadhyaya, Y. Fan, J. Zhao, M. Wang, L.-T. Chang, M. Lang, K. L. Wong, M. Lewis, Y.-T. Lin, J. Tang, S. Cherepov, X. Zhou, Y. Tserkovnyak, R. N. Schwartz, and K. L. Wang, "Direct imaging of thermally driven domain wall motion in magnetic insulators," *Phys. Rev. Lett.*, vol. 110, p. 177202, Apr 2013. [Online]. Available: http://link.aps.org/doi/10.1103/PhysRevLett.110.177202

[41] R. L. Cooper and E. A. Uehling, "Ferromagnetic resonance and spin diffusion in supermalloy," *Phys. Rev.*, vol. 164, pp. 662–668, Dec 1967.

[42] S. Zhang and S. S.-L. Zhang, "Generalization of the Landau-Lifshitz-Gilbert equation for conducting ferromagnets," *Phys. Rev. Lett.*, vol. 102, p. 086601, Feb 2009.

[43] C. Petitjean, D. Luc, and X. Waintal, "Unified drift-diffusion theory for transverse spin currents in spin valves, domain walls, and other textured magnets," *Phys. Rev. Lett.*, vol. 109, p. 117204, Sep 2012.

[44] K.-J. Lee, M. Stiles, H.-W. Lee, J.-H. Moon, K.-W. Kim, and S.-W. Lee, "Self-consistent calculation of spin transport and magnetization dynamics," *Physics Reports*, vol. 531, no. 2, pp. 89 – 113, 2013.

[45] J. Mendil, P. Nieves, O. Chubykalo-Fesenko, J. Walowski, T. Santos, S. Pisana, and M. Mnzenberg, "Resolving the role of femtosecond heated electrons in ultrafast spin dynamics," *Scientific Reports*, vol. 4, p. 3980, 2014.